CALCULATION OF CRITICAL EXPERIMENT PARAMETERS FOR THE HIGH FLUX ISOTOPE REACTOR*

CONF-920308--7

DE92 004232

R. T. Primm, III
Oak Ridge National Laboratory
P.O. Box 2008, Bldg. 6025, MS-6363
Oak Ridge, Tennessee 37831-6363

Submitted for publication in the *Proceedings* of the 1992 Reactor Physics Topical Meeting, Charleston, South Carolina, March 8–11, 1992.

*Managed by Martin Marietta Energy Systems, Inc., under contract DE-AC05-840R21400, U.S. Department of Energy.

CALCULATION OF CRITICAL EXPERIMENT PARAMETERS FOR THE HIGH FLUX ISOTOPE REACTOR

R. T. Primm, III
Oak Ridge National Laboratory
Oak Ridge, Tennessee 37831-6363
(615)574-0566

ABSTRACT

Six critical experiments were performed shortly before the initial ascension to power of the High Flux Isotope Reactor (HFIR). Critical configurations were determined at various control rod positions by varying the soluble boron content in the light water coolant. Calculated k-effective was 2% high at beginning-of-life (BOL) typical conditions, but was 1.0 at end-of-life (EOL) typical conditions. Axially averaged power distributions for a given radial location were frequently within experimental error. At specific r,z locations with the core, the calculated power densities were significantly different from the experimentally derived values. A reassessment of the foil activation data seems desirable.

INTRODUCTION

The HFIR is a beryllium reflected, light-water cooled, high-enriched uranium fueled reactor. The fuel elements consist of two concentric rings having a fueled height of 50.8 cm, an outer radius of 21 cm and an inner radius of 7.1 cm. The rings are composed of 1.27 mm thick, Al clad plates bent into the shape of an involute of a circle. A uniform, 1.27 mm thick water gap exists between plates. The initial approach to critical was in 1965.

As a part of establishing the operating limits for the HFIR, a set of six critical experiments were performed shortly before the initial ascension to full power. The HFIR reactor physics report (Ref. 1) includes a description of the experiments with the following statement of objectives. "These experiments, referred to as the HFIRCE-4 experiments, were performed to (1) investigate small differences (between previous criticals) and the HFIR overall core assemblies, (2) obtain more detailed power-distribution data, (3) calibrate the control rods, and (4) investigate more thoroughly the question of reproducibility."

All experiments were critical. Variation in control rod height for the six experiments was achieved by the addition of soluble boron to the light water coolant. All but one of the experiments had a simulated water target in the central island of the reactor. The final experiment had a target believed at the time to accurately approximate the neutron absorption in the planned Pu-242 target rods.

The local power densities were determined through activation of uranium foils. The foils were counted in a gamma ionization chamber with a counting accuracy of +-1%. "Performance of multiple irradiations indicated that the accuracy of the relative power distribution was about 5% (97% of the points agree within +-5%)." (Ref. 1) Power distribution data for a 1 cm (radial) by 2 cm (axial) grid are provided in Ref. 1 for each critical experiment. The power distributions are interpolations between or extrapolations from the locations with activated foils. Some foils were circular with a surface area of 0.5 cm**2; others rectangular with a length of 6.35 cm and a width of 0.16 cm..

CROSS SECTION PROCESSING

Before physics parameters can be calculated, nuclear data must be processed into a usable format. A description of the nuclear data source and the computer programs used to process the data follows. The processing models are described to a sufficient degree so as to allow for recreation of the few group library should that be necessary. Finally, a discussion is given of the few group library which is the end product of the cross section processing procedure.

NUCLEAR DATA LIBRARY

The starting point for nuclear data preparation is the 39 group ANSL-V General Purpose Neutron library (Ref. 2). All of the data extracted from this library for use in the HFIR calculations were derived from data from the Evaluated Nuclear Data File/B - Version V (ENDF/B-V, Ref. 3). The procedure by which ENDF/B-V data were collapsed to the 39 group structure is described in Ref. 2.

The 39 group library is in what is termed "AMPX master format". This means that each nuclide in the library must be processed further to obtain correct cross section values for the unresolved and resolved resonance regions for that nuclide. A description of the AMPX master format is contained in Ref. 2.

COMPUTER PROGRAMS USED TO PROCESS NUCLEAR DATA

All programs described in this section are modules of the AMPX system (Ref. 4). However, better documentation of the programs and required input can be found in Ref. 5.

The first program executed is the AJAX module. The sole purpose of this step is to extract only those nuclides from the library which are to be used in modeling the HFIR reactor. A new AMPX master library is created which will be used in subsequent steps. By creating a small subset of the original 39 group library some computational time is saved in succeeding steps.

The second program executed is the BONAMI module. The purpose of this step is to generate correct cross section values for the unresolved resonance energy range (see Ref. 5). The algorithm to accomplish this task is simple. First, the infinitely dilute values of the various reactions are computed for each nuclide. Then "Bondarenko factors" are determined by calculating each nuclide's cross section as a function of "background" cross section and generating the ratio of that value to the infinitely dilute value. By generating cross sections corresponding to several background cross section values and for several temperatures, a table can be constructed and interpolation used to determine intermediate values.

The BONAMI step and the two succeeding steps require some identification of a "unit cell". This unit cell geometry is input directly into the BONAMI and XSDRNPM (described subsequently) steps and indirectly into the NITAWL (described next) step.

For a conventional power reactor, a unit fuel cell is defined as a single fuel pin and its surrounding water channel. The analogy for HFIR would be to select a single involute plate and its associated water channel. However this assumption would be incorrect due to the small size of the HFIR core.

In a power reactor, the external dimensions of the reactor core are very large compared to the diameter of a fuel pin (several hundred times larger). But for the HFIR, the thickness of the fuel region of the annular core is only about 140 mm. The escape probability for a neutron born in the HFIR is much, much greater than for one born in a power reactor core. Indeed, the purpose of the HFIR is to leak neutrons to the central region where they may be absorbed in target rods.

The neutron spectra in the core is dominated by the thermal neutrons returning from the beryllium reflector. It is noted in Ref. 1 that the homogenization of fuel, clad and coolant is acceptable since the thermal flux depression from coolant centerline to fuel centerline is only 6.8%. Consequently, for the HFIR, the "unit cell" is the entire reactor.

For the BONAMI step, a cylindrical, four zone problem was created. The inner zone was a homogenized HFIR target. Surrounding this region was a representative fuel region with only trace amounts of fission products. Adjacent to the fuel was a control region. The outermost region was beryllium.

The target region actinide composition is shown in Table 1. Table 1 is based on data for Transuranium Facility campaign 65 (January, 1986) supplied by C. W. Alexander, ORNL.

Table 1. HFIR Target Rod Initial Composition

Nuclide	Grams	Unit Cell Atom Density (atoms per barn*cm)
Pu238	0.00111	2.23946e-8
Pu239	0.00060	1.20546e-8
Pu240	0.21320	4.26554e-6
Pu241	0.00002	3.98485e-10
Pu242	0.00057	1.13099e-8
Am241	0.0459	9.14522e-7
Am243	0.1463	2.89092e-6
Cm244	4.5730	8.99933e-5
Cm245	0.0656	1.28569e-6
Cm246	3.1523	6.15306e-5
Cm247	0.0889	1.72823e-6
Cm248	0.5507	1.06626e-5
Cf252	0.000015	1.85818e-10

The pellets in the target rods are 0.632 cm in diameter and are assumed to be clad with 0.24 cm thick Al-6061. The pins are located on a triangular pitch of 1.689 cm. Appropriate atom densities

for the constituents of water and Al-6061 were included with the smeared actinide atom densities in the BONAMI model.

One other input to the BONAMI model is the Dancoff (rod shadow) factor. Continuing the argument made previously, since the whole core is the unit cell, the Dancoff factor must be calculated for the whole core. In most instances, the Dancoff factor for a one lump object is 0.0. However the annular geometry for the HFIR means that there is some probability that a neutron entering the central target region will pass through and cause a fission on the "other side" of the annulus.

The CSAS1 module of the SCALE system (Ref. 5) was used to determine the Dancoff factor of an annulus having the same homogenized fuel region atom densities as the HFIR but with water in the central target region. The calculated Dancoff factor was 0.001774 and this value was input to the BONAMI program. Note that this exceptionally low value indicates that the annulus acts as if it were a single lump.

The third step in cross section processing is to execute the NITAWL module to properly process the resolved resonance energy region for those nuclides which have resolved resonances. With the exception of the uranium isotopes, all actinides are assumed to be present in "infinitely dilute" quantities. Likewise certain alloying agents in Al-6061 which have resolved resonance data are assumed to have infinitely dilute concentrations. The uranium isotopic ratios are assumed to be typical values from those reported in Ref. 1. The NITAWL model is based on the Nordheim integral treatment for a homogeneous annulus.

It is in the NITAWL step that the temperature of the nuclide is used to select appropriate scattering data and correctly doppler broaden the cross section resonances. All of the target actinides and all of the fuel nuclides and fission products are assumed to have a temperature of 430 degrees Kelvin. The water coolant, structural materials and beryllium reflector are all assumed to have a temperature of 343 degrees Kelvin. Note that the master cross-section library contains nuclear data only at certain temperatures. The NITAWL code selects data at a temperature closest to that entered by the user. No interpolation is performed.

The final step in the cross section processing procedure is to execute the XSDRNPM program. XSDRNPM is a one-dimensional, discrete ordinates solution to the Boltzman transport equation. The model input to XSDRNPM is the same as that shown in Table A.6 of Ref. 1 except for two changes.

The central target zone was modified to be three zones with smeared atom densities corresponding to the current target configuration. The innermost zone corresponded to the hydraulic irradiation tube. The second zone represented the 15 curium target rods. The third zone represented the 16 irradiation positions (assumed to be Al tubes).

The second change was to split the control rod zone into two regions. This allowed for representation of both the europium "black" and the tantalum "grey" regions in the same model. A k-effective calculation was performed with XSDRNPM using a buckling factor corresponding to the geometric height of the fueled region of the core (50.8 cm + extrapolation distance). The calculated value was 1.0691.

Forcing the calculated k-effective value to be 1.00 would have required a buckling height less than the physical height. However, the buckling factor for the thermal group is negative - flux peaking outside the core. For the epithermal and fast groups, it is likely to be close to the geometric

buckling. Since the better procedure of having group dependent buckling is not available in XSDRNPM, the buckling height was set to the geometric height.

The 39 group cross section set was collapsed to a 7 group set with the energy boundaries shown in Table 2. The selection of these boundaries is based on parametric studies performed as a part of the design of the Advanced Neutron Source reactor (Ref. 6).

Table 2. Group Structure for 7-Group Cross Section Library

Group Number	Upper Energy Boundary
1	20.0 MeV
2	100 keV
3	100 eV
4	0.625 eV
5	0.33 eV
6	0.162 eV
7	0.0300 eV
	0.00001 eV

In order to calculate temperature coefficients of reactivity, it is necessary to have cross-section data at elevated temperatures. Specifically, hydrogen datasets are needed at multiple temperatures. The same calculational sequence was used for the generation of elevated temperature datasets. Alternate temperature values were specified in the BONAMI and NITAWL datasets and the group collapse performed using the existing XSDRNPM dataset.

REACTOR ANALYSIS

The BOLD-VENTURE system for nuclear reactor analysis was used to determine k-effectives, fluxes, and power distributions (Ref. 7). The VENTURE diffusion theory module of the system had, as input, an R - Z model created with 17 annular fuel zones, target, reflector and control blade regions. The input to the VENTURE system was based on data provided in Figs. A.8 through A.10 and Table A.6 of Ref. 1. This section will present those parts of the input dataset which differed from the description given in Ref. 1.

FUEL REGION

Deviating from the description in Ref. 1, the fuel element sideplates were explicitly represented in the VENTURE model. Also, the atom densities for the constituents of the fuel zones were based on Al-6061 rather than pure Al. Both the Al filler and fuel plate clad were assumed to be Al-6061. The atom densities for the boron and uranium isotopes were calculated from Figs. A.9 and A.10 (schematic drawings of the inner and outer fuel plates respectively) and compared to values given in Table A.6 of Ref. 1. Agreement was excellent (usually within 1%). The total quantity of U-235 as tallied from the input was found to be 9.46 Kg. The value quoted in Ref. 1 is 9.40 Kg.

The radial mesh in the VENTURE model was the same as that noted in Table A.6 of Ref. 1. The axial mesh varied according to the critical experiment being modeled; the control blade position varying according to coolant boron loading for a given critical experiment.

CONTROL BLADES

In Ref. 1, the outer element sideplate and inner control blade and water gap between these structures were all homogenized into one region. In the VENTURE model these structures were represented separately. However, for the control blade, the Al clad was homogenized with the control poison material.

The "black" control material reported in Table A.6 of Ref. 1 is boron. The actual control blades used in the HFIRCE-4 experiments had europium in this region. The VENTURE model contains atom densities corresponding to the europium oxide - tantalum - Al design (still the current HFIR configuration). The dimensions and content of the control blade were supplied by R. W. Hobbs, Research Reactors Division.

Initial calculations of experiments with the control rod fully inserted yielded unusually low values of calculated k-effective. The nuclear data for the control region was examined and the diffusion coefficient for the europium region was modified via a procedure described in Appendix A. All calculated k-effective values reported here are for models incorporating the modified europium diffusion coefficient.

RESULTS OF CALCULATIONS

The calculated values of k-effective are shown in Table 3. The best agreement between calculation and experiment is seen in the "cleanest" core configuration (blades out). At this point, agreement is -0.3%. The worst case is with control blades fully inserted and a water target - agreement being 2.2%.

Table 3. Calculated k-effectives for HFIR Critical Experiments

Expt. No.	Control Blade Position (cm)	Boron Conc. in Coolant (g per L)	Target Material	k-effective
4.1	44.45	0.0	water	1.0219
4.2	49.28	0.527	water	.9872
4.3	54.09	0.910	water	.9872
4.4	61.72	1.25	water	.9890
4.5	67.31 (out)	1.35	water	.9967
4.6	42.16	0.0	sim. Pu	1.0206

The source of the discrepancy at beginning-of-life typical conditions (2%) is unknown. By comparison of cases 4.1 and 4.6, it would appear that the source of the discrepancy is independent of target material. The calculational bias changes sign as the control blade is withdrawn and then approaches 1.0. Based on the assumption that the 67.31 cm rod position represents end-of-life, there should be no bias applied to actual reactor calculations when attempting to determine cycle length for a given reactor configuration.

The effect on k-effective of varying the number of mesh points in the fuel is shown in Table 4. For all cases examined, there is a slight increase in calculated k-effective (0.002 to 0.004) as the number of mesh points in the fuel is increased. However, the previously identified discrepancies remain largely unchanged.

Table 4. Effect of Mesh Point Spacing on Calculated K-effectives

	Mesh Points in Fuel		
Expt. No.	R	Z	K-effective
4.1	19	30	1.022
4.1	68	78	1.026
4.2	19	34	0.987
4.2	68	63	0.989
4.5	19	30	0.997
4.5	68	78	1.000
4.6	19	30	1.021
4.6	68	86	1.024

HFIR procedures stipulate that any change/addition to the irradiation positions must be certified to cause no more than a 5% increase in local power density at any given position in the reactor. Frequently this certification is made by comparison to previously performed experiments. For new materials or designs, certification must rely on computations.

Comparisons of calculated and experimentally derived local power densities for each of the six critical experiments are given in Figs. 1 and 2. The description of the experiments, the measurement procedure, some of the experimental data, and all of the experimentally derived local power densities are contained in Ref. 1.

As the control blades are withdrawn (Expts. 4.1 - 4.5), the power densities in the inner element change from being generally overpredicted to being underpredicted. Likewise, as the blades (located outside the outer element) are withdrawn, the power densities at the outside edge of the outer element are overpredicted and those at the inside edge are underpredicted.

For convenience, the locations and values of the maximum point power densities are contained in Table 5. Also shown there are the locations and values of the greatest percentage difference by which the experimentally measured local power density exceeds the calculated value. The former is important because of safety considerations related to the "hot spot" power density. The latter is important for determining maximum bias factors which could be applied to calculations to insure conservatism regarding thermal-hydraulic limits.

The impact on calculated power distribution of increasing the number of mesh points was studied for experiment 4.6, the fine mesh calculation exhibits poorer agreement with experiment. The fine mesh calculation appears to yield a more strongly buckled flux distribution than experimental measurements yield.

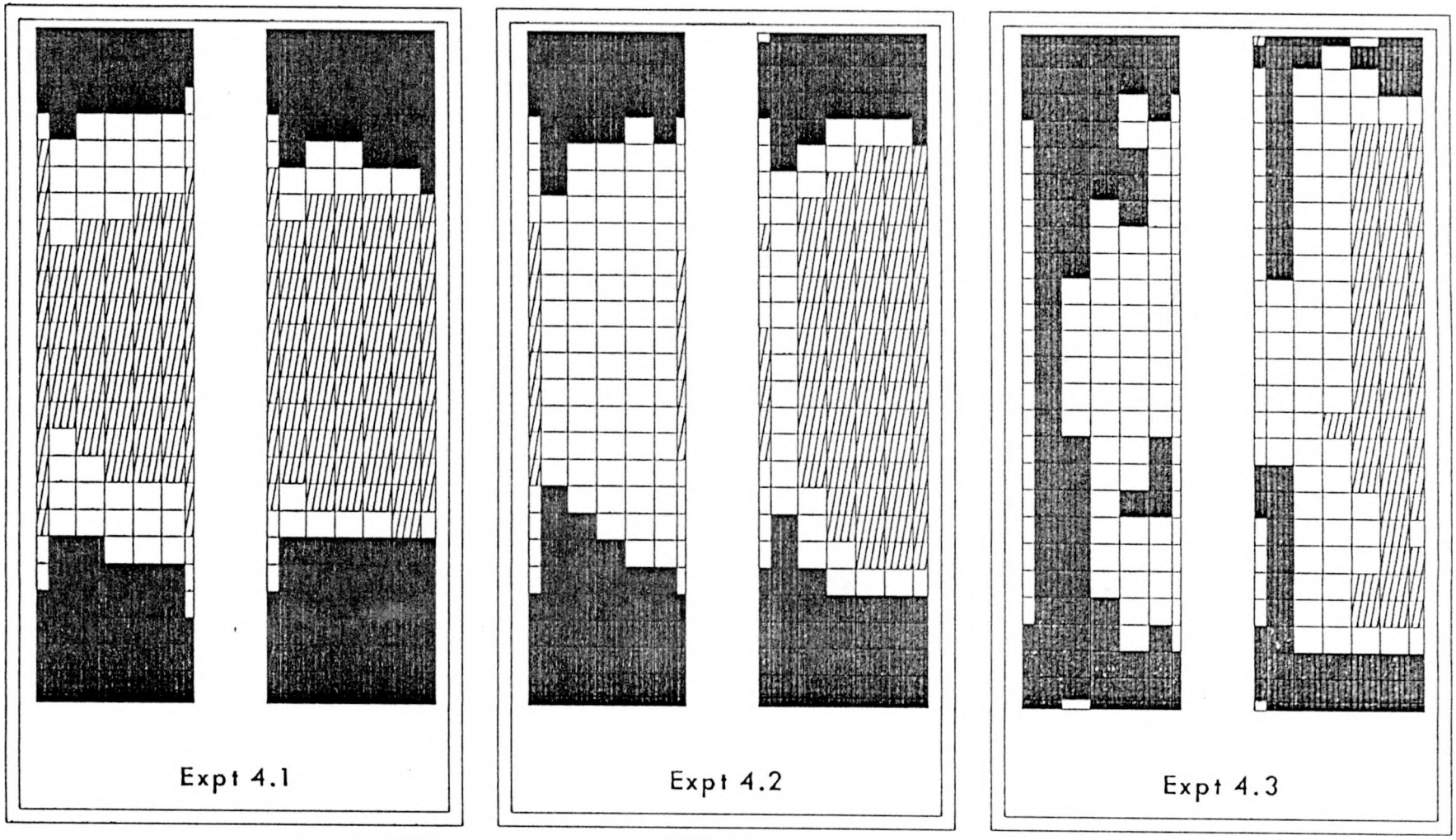

Fig. 1 Comparisons of calulated and measured power densities for HFIR critical experiments; inner element at left, outer at right; light shade = undercalculate by more than 5%, dark shade = overcalculate by more than 5%.

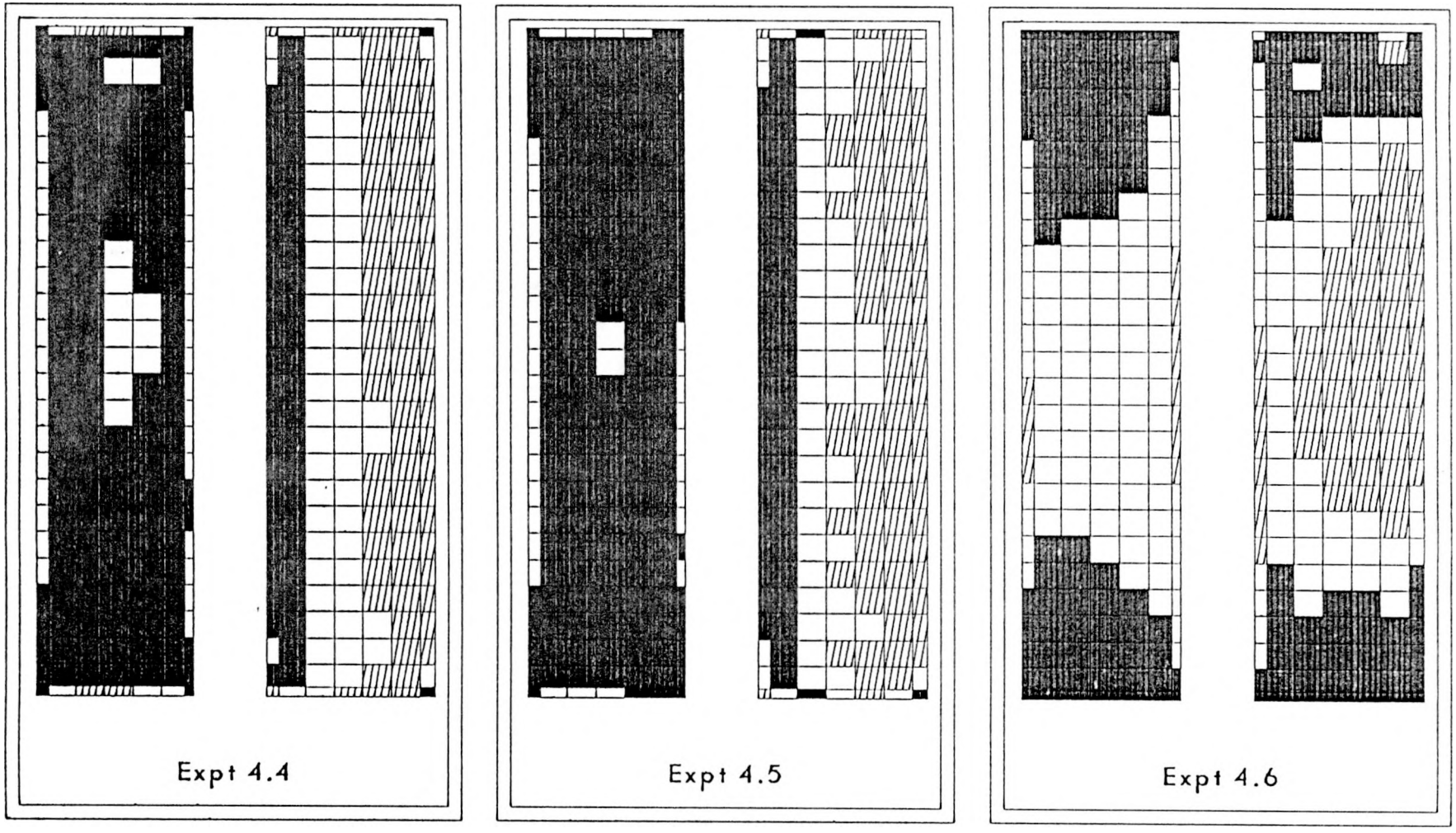

Fig. 2 Additional comparisons of calulated and measured power densities for HFIR critical experiments; inner element at left, outer at right; light shade = undercalculate by more than 5%, dark shade = overcalculate by more than 5%.

Table 5. Peak Power Locations for Critical Experiments

	Max. Relative Power Density			Max. % Expt. Over Calc.		
		Location (cm)			Location (cm)	
Expt. No.	Value	Radial	Axial	Value	Radial	Axial
4.1	2.38	17.00	25.40	34.69	21.00	2.00
4.2	1.64	7.14	0.00	29.29	21.00	4.00
4.3	1.62	7.14	0.00	22.66	20.00	16.00
4.4	1.56	7.14	0.00	19.04	21.00	18.00
4.5	1.50	7.14	0.00	17.66	21.00	-8.00
4.6	2.11	10.00	25.40	30.50	21.00	-4.00

For calculation of margin to incipient boiling, the key parameter of interest is the quantity of energy deposited in the water coolant as it flows downward through the core. Consequently, it is desirable to accurately estimate the quantity of heat generated along any axial pathway inside the core. Table 6 provides a comparison of experimentally measured and calculated, axially averaged relative power densities for each of the six critical experiments. In almost all cases, the level of agreement is within the experimental uncertainty (5%).

The accuracy of calculated local power densities for these critical experiments is summarized in a slightly different manner in Table 7. The second column in the table contains the calculation-to-experiment (c/e) ratio for the point in the core at which the percentage by which the experimental value exceeds the calculated value is largest. That is, the point at which the computational method would most underpredict the power on a percentage basis. The third and fourth columns provide data for the hottest axial coolant path in the core. The third column shows the axially averaged c/e ratio. The fourth column shows c/e ratios for the point in the hottest axial path at which the computational method would most underpredict the power on a percentage basis.

The variation in the max. local c/e ratio for whole core casts some doubt on the ability to accurately determine the worth of a perturbation. A reassessment of the manner in which the irradiated foil data were transformed to power density maps seems desirable since no details of the procedure are contained in Ref. 1. A significant impact on experiment/ calculation agreement could occur depending on the procedure used to count the foil activity. Since the length of these foils is greater than the mesh spacing for which the experimentally derived data is reported, the manner in which the foils were analyzed (cut into pieces or measured whole) must be known to correctly interpret the values reported in Ref. 1.

Table 6. Comparison of Experimental and Calculated Axially Averaged Relative Power Densities
100*(Expt.-Calc.)/Expt.

	Experiment Number					
Radius (cm)	4.1	4.2	4.3	4.4	4.5	4.6
7.14	4.56	.66	-.25	-4.31	-5.09	-2.88
8.0	-4.80	-9.06	-10.14	-15.82	-15.70	-9.37
9.0	-2.48	-6.29	-7.49	-10.73	-12.38	-6.70
10.0	-.26	-3.58	-4.18	-6.11	-8.05	-6.00
11.0	.91	-2.39	-3.82	-6.12	-7.80	-4.72
12.0	.55	-4.07	-5.25	-9.35	-10.79	-3.30
12.6	5.70	-.61	-.34	-5.16	-7.02	2.58
15.15	3.32	-.63	-3.77	-8.09	-7.28	3.03
16.0	-3.59	-6.15	-6.52	-8.54	-8.54	-4.91
17.0	-.51	-.38	.13	.07	.40	-.93
18.0	-.76	2.41	2.22	3.19	4.30	2.20
19.0	-1.64	4.75	5.40	6.78	6.06	6.23
20.0	-1.58	9.67	11.19	12.27	11.93	14.16
21.0	-6.76	10.42	9.41	14.67	14.70	14.17

Table 7. Local Power Density Ratios for HFIR Critical Experiments

	Calculation-to-Experiment Ratio		
		"Hot Streak"	
Control Blade Position (cm)	Max. Local for Whole Core	Axial Ave.	Max. Local
42.16	0.695	1.029	0.944
44.45	0.653	0.954	0.838
49.28	0.707	0.993	0.910
54.09	0.773	1.002	0.966
61.72	0.810	1.043	0.991
67.31 (out)	0.823	0.853	0.823

While the worst position for the whole core has a c/e ratio much lower than desired (experimental error +-5%), the axially averaged values for the hot streak are acceptable in all but one case. However, the 67.31 cm case is the only critical configuration in which the "hot streak" lies along the outside edge of the outer fuel element. This region lies at the point of transition between a weakly absorbing region (Be, Al, water) and a strongly absorbing region (highly enriched uranium). The assumptions underlying diffusion theory would be least applicable at that point in the model.

The ability to accurately calculate axially averaged power densities is important because the temperature at the exit of the "hot streak" determines the margin to incipient boiling and therefore the maximum steady-state overpower limit. These calculations indicate that reactor physics calculation input to the thermal-hydraulic computer codes should yield accurate (within experimental uncertainties) "hot streak" exit temperatures for all except the "rods full out" position. At that configuration, a bias of 15% should be applied.

CONCLUSIONS

HFIR specific, few group neutron and coupled neutron-gamma libraries have been prepared. These are based on data from ENDF/B-V and beginning-of-life (BOL) conditions. The neutron library includes actinide data for curium target rods. In previous calculations reported in 1971, only simulated Pu-242 target data were utilized.

Six critical experiments, collectively designated HFIR critical experiment 4, were analyzed. Calculated k-effective was 2% high at BOL-typical conditions but was 1.0 at end-of-life-typical conditions. These results indicated that if exposure related parameters can be estimated accurately, an accurate estimate of cycle length should be attainable.

Through studies of the critical experiments, it was determined that a special blackness treatment was required in order to obtain correct diffusion coefficients for the europium regions of the control blades. Nevertheless, the variance in k-effective as a function of control blade position indicated that reviews of the exact positions of the control blades and the exact boron concentrations in the coolant were needed.

The local power density distributions were calculated for each of the critical experiments. The axially averaged values at a given radius were frequently within experimental error. However at individual points, the calculated local power densities were significantly different from the experimentally derived values (several times greater than experimental uncertainty). A reassessment of the foil activation data seems desirable.

One potential use of diffusion calculations is in the certification of reactor experiments. It is required that a given experiment will not change any local power density by more than 5%. The critical experiment calculations indicate that only certain experiments could be certified using diffusion theory.

If the reactivity worth of the experiment is small (control blade movement less than a centimeter), then unperturbed and perturbed distributions could be compared to determine percentage difference. However, if the pre- and post-experiment-insertion control blade positions are significantly different, then the differences in the power distributions among the critical experiments indicates that an effect due to the experiment would not be quantifiable. This is due to differences in calculation/experiment agreement for a given physical position among the critical experiments usually exceeding 5%. Again, a reassessment of foil activation data could modify this conclusion.

REFERENCES

1. R. D. Cheverton and T. M. Sims, "HFIR Core Nuclear Design," ORNL-4621 (July 1971).

2. W. E. Ford, III, et al., "ANSL-V: ENDF/B-V Based Multigroup Cross-section Libraries for Advanced Neutron Source (ANS) Reactor Studies," ORNL-6618 (September 1990).

3. R. Kinsey, ed., "ENDF/B Summary Documentation," BNL-NCS-17541 (ENDF-201), 3rd ed., Brookhaven National Laboratory (1979).

4. N. M. Greene, et. al., "AMPX: A Modular Code System for Generating Coupled Multigroup Neutron-Gamma Libraries from ENDF/B," ORNL-TM-3706 (March 1976).

5. "SCALE: A Modular Code System for Performing Standardized Computer Analyses for Licensing Evaluation, Vols. 1-3," NUREG/CR-0200, U.S. Nuclear Regulatory Commission (originally issued July 1980, reissued January 1982, Rev. 1 issued July 1982, Rev. 2 issued June 1983, Rev. 3 issued December 1984).

6. R. T. Primm, III, "Accuracy of Calculated Power Distribution Using Few Group Cross-Section Sets," Trans. Am. Nucl. Soc., Vol. 61 (June 1990).

7. D. R. Vondy, T. B. Fowler, and G. W. Cunningham, III, "The Bold Venture Computation System for Nuclear Reactor Core Analysis, Version III," ORNL-5711 (June 1981).

8. A. F. Henry, Nuclear Reactor Analysis, The MIT Press, pp. 433-454 (1975).

APPENDIX A

Equivalent Diffusion Theory Coefficients Derived From Transport Theory Calculations

Initial calculations of the six critical experiments showed that those in which the control blades were fully or nearly fully withdrawn yielded k-effectives close to 1.0. However, those in which the control blades were inserted yielded k-effectives which were low (0.9). After verifying the model input regarding control blade position and boron content in the coolant, it was suspected that the diffusion coefficients as generated by the computational procedure were in error. A procedure by A. F. Henry (Ref. 8) for dealing with bladed control rods was employed to derive new diffusion coefficients.

Henry states, "for the one dimensional case, we use the fact that parameters which preserve all the integrated reaction rates within all subregions V_i must necessarily preserve the net leakage rate out of each V_i.... In slab geometry (or in this case, annular geometry in which the height >> thickness of the annulus) this extra restriction implies that, if we know from more accurate calculations (in this case discrete ordinates calculations from XSDRNPM) the column vector $J(r_i)$ of group currents at the point x_i separating a zone of thickness Δ_{i-1} from its neighbor of thickness Δ_i, we want the equivalent diffusion-theory parameters for these zones to be such that solution of the group diffusion equations containing the effective constants will reproduce the $J(r_i)$. If we also require that the column vector of group fluxes $\Phi(r_i)$ at all the interfaces match those values known from more accurate calculations (again, discrete ordinates calculations using XSDRNPM), a systematic procedure for finding the equivalent parameters emerges."

"We consider first the one-group case with the material inside Δ_i homogeneous but not of a nature such that diffusion theory should be valid." In this case, a control blade with no annular or axial (height >> thickness) variation. If equivalent constants $\overline{v\sum_f}$, $\overline{\sum_a}$, and $\overline{D}$ can be found for this case, they will be such that within Δ_i the one-group P_1 equations are

$$\frac{d}{dr}J(r) + \overline{\sum_a}\Phi(r) = \overline{v\sum_f}\Phi(r),$$

$$\frac{d}{dr}\Phi(r) + \frac{1}{\overline{D}}J(r) = 0.$$

Note that for this problem $\overline{v\sum_f} = 0$. Also note, that the above equations are applicable to the multigroup solution if we assume that there is no scattering between groups. Given the seven-group energy structure and the fact that the control blades are composed of europium (atomic number = 63) this is a good assumption.

In matrix form these become:

$$\frac{d}{dr}\begin{bmatrix}\Phi\\ J\end{bmatrix} = -\begin{bmatrix}0 & \frac{1}{\overline{D}}\\ \overline{\sum}_a & 0\end{bmatrix}\begin{bmatrix}\Phi\\ J\end{bmatrix}, \tag{1}$$

and, with the definitions:

$$[u(r)] \equiv \begin{bmatrix}\Phi(r)\\ J(r)\end{bmatrix}, \qquad [N] \equiv \begin{bmatrix}0 & \frac{1}{\overline{D}}\\ \overline{\sum}_a & 0\end{bmatrix}$$

(1) becomes

$$\frac{d}{dr}[u(r)] + [N][u(r)] = 0\,. \tag{2}$$

The solution to this equation is given in Ref. 8 and is shown to be

$$\begin{bmatrix}\Phi(r_{i+1})\\ J(r_{i+1})\end{bmatrix} = \begin{bmatrix}\cosh\kappa\Delta & -(\overline{D}\kappa)^{-1}\sinh\kappa\Delta\\ -\overline{D}\sinh\kappa\Delta & \cosh\kappa\Delta\end{bmatrix}\begin{bmatrix}\Phi(r_i)\\ J(r_i)\end{bmatrix}.$$

where the subscripts i, i+1 represent intervals in the problem and $\kappa^2 = \frac{\overline{\sum_a} - \overline{\upsilon\sum_f}}{\overline{D}} = \frac{\overline{\sum_a}}{\overline{D}}$.

Defining blackness coefficients α and β by

$$\alpha \equiv \frac{J(r_i) - J(r_{i+1})}{\Phi(r_i) + \Phi(r_{i+1})}, \qquad \beta \equiv \frac{J(r_i) + J(r_{i+1})}{\Phi(r_i) - \Phi(r_{i+1})},$$

it can be shown that

$$\sinh\kappa\Delta = \sqrt{(\cosh^2\kappa\Delta - 1)} = \frac{2\sqrt{(2\beta)}}{\beta - 2}$$

and

$$\overline{D} = \frac{1}{\kappa}\sqrt{(\alpha\beta)}$$

For the calculations described in this document, multigroup flux and current values for mesh points on the front and rear faces of the control blade were used to define α and β. The group diffusion coefficients were then determined directly.

The VENTURE neutronics module has an input option whereby two constants, a and b, can be entered and the value of the diffusion coefficients, for a given zone, as calculated from the cross-section data library are modified according to the formula

$$\text{new diffusion coefficient} = a\ (\text{old diffusion coefficient}) + b$$

The diffusion coefficients for the europium region of the control rod were compared to the "old" values derived from the data library and could be linearly correlated with a correlation coefficient R^2, equal to 0.998. The value of a was determined to be 0.01937 and the value of b was determined to be 0.001665.